

Extended impurity potential in a $d_{x^2-y^2}$ superconductor

A. P. Kampf

Institut für Theoretische Physik, Universität zu Köln, Zùlpicher Strasse 77, 50937 Köln, Germany

T. P. Devereaux

Department of Physics, George Washington University, Washington, D.C. 20052

(Received 18 February 1997)

We investigate the role of a finite potential range of a nonmagnetic impurity for the local density of states in a $d_{x^2-y^2}$ superconductor. Impurity-induced subgap resonances are modified by the appearance of further scattering channels beyond the s -wave scattering limit. The structure of the local density of states (DOS) in the vicinity of the impurity is significantly enhanced and therefore improves the possibility for observing the characteristic anisotropic spatial modulation of the local DOS in a $d_{x^2-y^2}$ superconductor by scanning tunneling microscopy. [S0163-1829(97)08530-5]

A lot of attention has been focused recently on the role of impurities in unconventional superconductors. The reason for this interest is that impurities modify the superconducting properties in a way which is characteristic for the pairing state and thereby serve as a diagnostic tool for its identification. In particular, magnetic impurities act as strong pair breakers for superconductors in a spin singlet pairing state while already nonmagnetic impurities are pair breakers in superconductors with a nontrivial phase of the pairing amplitude. The latter kind of defects or impurities have only little effect on the transition temperature and the superfluid density in conventional s -wave superconductors as understood from Anderson's theorem.¹

Regarding high- T_c superconducting materials evidence has accumulated for an anisotropic energy gap most likely of $d_{x^2-y^2}$ symmetry.² For this pairing state nonmagnetic impurities produce a finite lifetime for quasiparticles near the nodes of the gap and a finite density of state (DOS) at low energies.³⁻⁵ Indeed, the measured low-temperature properties of high- T_c materials show a remarkable sensitivity for impurity effects. Examples are the T^2 variation of the low-temperature penetration depth⁶ and the Knight shift in Zn-doped Y-Ba-Cu-O,⁷ and the ω^3 to ω crossover in the low frequency B_{1g} Raman intensity.⁸

A general feature of pair breaking impurities in s -wave superconductors is that they lead to bound quasiparticle states in the energy gap.⁹ Similarly, for a d -wave superconductor with a particle-hole continuum and a DOS extending linearly to zero frequency, low energy resonances are created with a highly anisotropic structure.¹⁰⁻¹² Increasing the impurity concentration these subgap resonances form bands which give rise to the aforementioned finite DOS at zero energy. The local structure of the resonant states in the vicinity of the impurity is characteristic of the pairing state of the superconductor. It has therefore been suggested that probing these impurity states by scanning tunneling microscopy (STM) offers a direct way for measuring the anisotropic structure of the pairing state.¹³ However, the predicted effect may be too small to detect with the current STM spatial resolution and thus any advances that could enhance a characteristic signal would be helpful towards making STM a feasible probe to detect the gap symmetry.¹⁴

Systematic studies in high- T_c materials have been performed by substituting Zn on the planar Cu sites and thereby suppressing the local moment. Model calculations, as initiated by the early work of Annett *et al.* and Hirschfeld and Goldenfeld,³ which assume a $d_{x^2-y^2}$ gap function with unitary s -wave impurity scattering have provided a consistent explanation for the experimentally observed transport properties. The origin of the unitary nature of this scattering from local defects has been ascribed to strong electronic correlations. While this issue is unsettled, it has in fact been suggested that a Zn impurity may not simply act as a local moment vacancy because it induces a magnetic moment in its surrounding in the CuO_2 planes.¹⁵

Transport data on Zn-doped metallic Y-Ba-Cu-O have furthermore been used to infer a spatially extended nature of the effective impurity potential. In particular, a scattering cross section diameter larger than the Cu-Cu distance has been deduced from the residual resistivity.¹⁶ Theoretically, for a model calculation of static vacancies in a Heisenberg antiferromagnet it has been shown early on that the ordered staggered magnetic moment is enhanced within a few lattice spacings around the vacancy.¹⁷ Therefore, even in the hole-doped system when spin correlations are dynamic and have a finite range the spatially extended structure of impurity effects is expected to persist. Electronic correlation effects thus provide a natural origin for the transport data.

A series of model studies has been performed in recent years on the properties of dirty d -wave superconductors. Most of the analytical studies have assumed s -wave impurity scattering while numerical simulations of impurities in Hubbard or t - J type models have in fact demonstrated the expected effective, dynamically generated finite impurity potential range.¹⁸ As a consequence higher order partial wave scattering channels become important and lead to resonances in each channel. Impurity models for cuprate superconductors thus need to take into account the extended nature of the scattering centers.^{5,19}

In this paper we explore the T matrix in a minimal, physically transparent extended impurity potential model in a d -wave superconductor. In a partial wave decomposition the single impurity problem is solved exactly. Subgap reso-

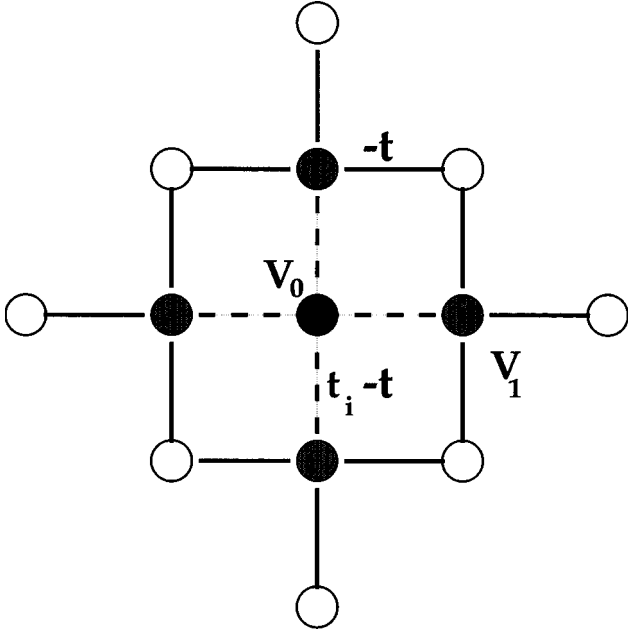


FIG. 1. Model for a nonmagnetic extended impurity on a square lattice. V_0 is the potential at the impurity center and V_1 the potential at the nearest neighboring (NN) sites; t_i is the change of the NN hopping amplitude of the host value $-t$.

nances in the local DOS are strongly enhanced by a finite range of the potential and may thus be the origin for the unitarity limit scattering which was favored in previous dirty d -wave studies for cuprate superconductors. This enhancement of the resonances improves the possibility for the detection of their highly anisotropic spatial structure in STM spectroscopy. Also the impurity-induced zero energy DOS is found to be significantly increased for finite impurity concentrations as compared to the s -wave scattering limit for a local impurity potential.

Specifically we model the scattering from impurity centers located at the sites $\{\mathbf{l}\}$ on a square lattice

$$H_i = \sum_{\{\mathbf{l}\}, \sigma, \delta} \left[\frac{V_0}{4} n_{\mathbf{l}, \sigma} + t_i (c_{\mathbf{l}, \sigma}^+ c_{\mathbf{l}+\delta, \sigma} + \text{H.c.}) + V_1 n_{\mathbf{l}+\delta, \sigma} \right] \quad (1)$$

(see Fig. 1). Here, δ connects to the nearest-neighbor sites, V_0 and $V_1 < V_0$ are potential strengths at the impurity center and its nearest-neighbor sites (NN), respectively, and t_i is an additional contribution to the NN hopping amplitude which we assume to be of opposite sign to the pure host value $-t$. By focusing on a two parameter model for the specific parameter relation $V_1 = \alpha^2 V_0/4$ and $t_i = \alpha V_0/4$ in Eq. (1) Fourier transformation leads to

$$H_i = \frac{V_0}{4N} \sum_{\mathbf{l}, \sigma} \sum_{\mathbf{k}, \mathbf{q}, \delta} e^{i(\mathbf{k}-\mathbf{q}) \cdot \mathbf{l}} V_{\mathbf{k}, \delta}^* V_{\mathbf{q}, \delta} c_{\mathbf{k}, \sigma}^+ c_{\mathbf{q}, \sigma}, \quad (2)$$

where $V_{\mathbf{k}, \delta} = 1 + \alpha e^{i\mathbf{k} \cdot \delta}$. The virtue of the parameter choice becomes apparent in the factorization of the scattering potential which allows for an algebraic solution of the single impurity T matrix. α is the control parameter for the extension of the potential to the NN sites. The single particle Green function in the presence of the impurity is

$\hat{G}(\mathbf{k}, \mathbf{k}', \omega) = \delta_{\mathbf{k}, \mathbf{k}'} \hat{G}^0(\mathbf{k}, \mathbf{k}', \omega) + \hat{G}^0(\mathbf{k}, \omega) \hat{T}_{\mathbf{k}, \mathbf{k}'}(\omega) \hat{G}^0(\mathbf{k}', \omega)$. All quantities are 2×2 matrices in Nambu particle-hole spinor space. The clean Green function is given by $[\hat{G}^0(\mathbf{k}, \omega)]^{-1} = \omega \hat{\tau}_0 - \Delta_{\mathbf{k}} \hat{\tau}_1 - \xi_{\mathbf{k}} \hat{\tau}_3 = [\sum_{i=0,1,3} \hat{\tau}_i g_i]^{-1}$, where $\hat{\tau}_i$ ($i=1,2,3$) are the Pauli matrices, $\hat{\tau}_0$ is the unit matrix, and $\xi_{\mathbf{k}}$ is the quasiparticle tight binding energy relative to the chemical potential. Specifically, we consider a superconductor with a $d_{x^2-y^2}$ gap function $\Delta_{\mathbf{k}} = \Delta(\cos k_x - \cos k_y)/2$.

In order to explore local properties in the vicinity of an impurity we consider first the problem of a single impurity located at the origin $\mathbf{l} = \mathbf{0}$. The momentum dependent T matrix is obtained from the set of equations:

$$\hat{T}_{\mathbf{k}, \mathbf{k}'}(\omega) = \frac{V_0}{4} \sum_{\delta, \delta'} V_{\mathbf{k}, \delta}^* \hat{t}_{\delta, \delta'} V_{\mathbf{k}', \delta'}, \quad (3)$$

$$\hat{t} = [\hat{\tau}_0 \mathbf{1} - \hat{\tau}_3 \hat{t}^0]^{-1} \hat{\tau}_3, \quad (4)$$

$$\hat{t}_{\delta, \delta'}^0 = \frac{V_0}{4} \sum_{\mathbf{k}} V_{\mathbf{k}, \delta} \hat{G}^0(\mathbf{k}, \omega) V_{\mathbf{k}, \delta'}^*, \quad (5)$$

where underlined quantities are 4×4 matrices with respect to the NN site coordinates next to the impurity center; note that their matrix entries contain noncommuting Pauli matrices and therefore the matrix inversion in Eq. (4) is nontrivial.

Using the square lattice basis functions $\gamma_{\mathbf{k}}^{(s/d)} = \frac{1}{2}(\cos k_x \pm \cos k_y)$ and $\gamma_{\mathbf{k}}^{(p1/p2)} = \frac{1}{2}(\sin k_x \pm \sin k_y)$ and thus decomposing into s -, p -, and d -wave scattering channels we obtain the algebraic result for the T matrix in the form

$$\hat{T}_{\mathbf{k}, \mathbf{k}'}(\omega) = V_0 \mathbf{U}_{\mathbf{k}}^* \hat{D}(\omega) \mathbf{U}_{\mathbf{k}}, \hat{\tau}_3, \quad (6)$$

$$\mathbf{U}_{\mathbf{k}} = [(1 + \alpha \gamma_{\mathbf{k}}^s), i\alpha \gamma_{\mathbf{k}}^{p1}, i\alpha \gamma_{\mathbf{k}}^{p2}, \alpha \gamma_{\mathbf{k}}^d],$$

where the matrix $\hat{D}(\omega)$ is given by

$$\hat{D}(\omega) = \begin{bmatrix} \hat{\tau}_1 \hat{d} \hat{\tau}_1 \hat{S}^{-1} & 0 & 0 & \hat{a}^+ \hat{D}^{-1} \\ 0 & \hat{\tau}_1 \hat{p} \hat{\tau}_1 \hat{P}^{-1} & \hat{a}^- \hat{P}^{-1} & 0 \\ 0 & \hat{a}^- \hat{P}^{-1} & \hat{\tau}_1 \hat{p} \hat{\tau}_1 \hat{P}^{-1} & 0 \\ \hat{a}^+ \hat{S}^{-1} & 0 & 0 & \hat{\tau}_1 \hat{s} \hat{\tau}_1 \hat{D}^{-1} \end{bmatrix}. \quad (7)$$

The structure of the matrix \hat{D} apparently implies a mixing of the s - and d - and the two p -wave scattering channels, respectively. The matrix elements in Eq. (7) are determined by the 2×2 matrix functions

$$(\hat{s}, \hat{p}, \hat{d}) = \hat{\tau}_0 - \frac{V_0}{4N} \sum_{\mathbf{k}} (s_{\mathbf{k}}, p_{\mathbf{k}}, d_{\mathbf{k}}) \hat{\tau}_3 (\hat{\tau}_0 g_0 + \hat{\tau}_3 g_3), \quad (8)$$

$$\hat{a}^{\pm} = \frac{V_0}{4N} \sum_{\mathbf{k}} a_{\mathbf{k}}^{\pm} \hat{\tau}_3 g_1 \hat{\tau}_1, \quad (9)$$

$$\hat{S} = \hat{s} \hat{\tau}_1 \hat{d} \hat{\tau}_1 - (\hat{a}^+)^2, \quad \hat{P} = \hat{p} \hat{\tau}_1 \hat{p} \hat{\tau}_1 - (\hat{a}^-)^2, \quad (10)$$

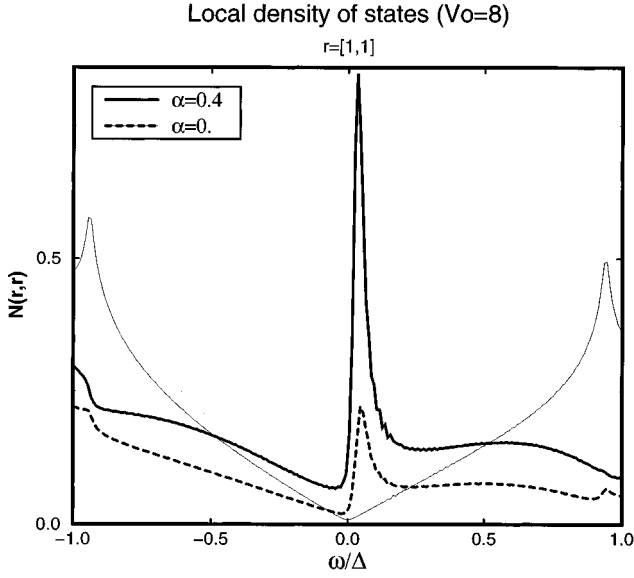


FIG. 2. Frequency dependence of the local DOS at $\mathbf{r} = (1,1)$ at $V_0 = 8t$ for an extended ($\alpha = 0.4$, bold solid line) and a local ($\alpha = 0$, dashed line) impurity in a $d_{x^2-y^2}$ superconductor. The impurity center is at the origin $\mathbf{r} = (0,0)$. The thin solid line shows the pure DOS.

$$\hat{D} = \hat{d}\hat{\tau}_1\hat{s}\hat{\tau}_1 - (\hat{a}^+)^2 \quad (11)$$

with the momentum dependent coefficients

$$s_{\mathbf{k}} = 4 + 2\alpha^2 + 8\alpha\gamma_{\mathbf{k}}^s + 4\alpha^2 \cos k_x \cos k_y - p_{\mathbf{k}},$$

$$d_{\mathbf{k}} = 2\alpha^2 - 8\alpha^2 \cos k_x \cos k_y - p_{\mathbf{k}},$$

$$p_{\mathbf{k}} = \alpha^2 - \frac{\alpha^2}{2}(\cos 2k_x + \cos 2k_y),$$

$$a_{\mathbf{k}}^{\pm} = 2\alpha\gamma_{\mathbf{k}}^d \pm \left[2\alpha\gamma_{\mathbf{k}}^d + \frac{\alpha^2}{2}(\cos 2k_x - \cos 2k_y) \right]. \quad (12)$$

In the limit $\alpha \rightarrow 0$ the T matrix becomes momentum independent and reduces to the known s -wave scattering result of a local impurity potential.²⁰ Note, however, that for finite α the T matrix $\hat{T} = \sum_{i=0}^3 T_i \hat{\tau}_i$ has components in $\hat{\tau}_0$ and all three Pauli matrices while $T_1 = T_2 = 0$ for $\alpha = 0$. Given the explicit algebraic solution of $\hat{T}_{\mathbf{k},\mathbf{k}'}(\omega)$ the local DOS then follows from

$$N(\mathbf{r}, \mathbf{r}, \omega) = \frac{-1}{\pi N^2} \text{Im} \sum_{\mathbf{k}, \mathbf{k}'} e^{-i\mathbf{k} \cdot \mathbf{r}} \hat{G}_{11}(\mathbf{k}, \mathbf{k}', \omega) e^{i\mathbf{k}' \cdot \mathbf{r}}, \quad (13)$$

with $\omega + i0^+$ implied.

We have evaluated the local DOS using a free tight binding band $\xi_{\mathbf{k}} = -4t\gamma_{\mathbf{k}}^s + 4t' \cos k_x \cos k_y - \mu$, with $t = 1$ as the energy unit and $t' = 0.4$, for a band filling $n = 0.86$ and a d -wave gap amplitude $\Delta = 0.3$. Yet, the conclusions are insensitive to changes in this parameter choice. The potential at the impurity center is chosen as twice the bandwidth $V_0 = 8$. All results for the extended potential, i.e., finite α , are compared to the local potential case $\alpha = 0$.

In Fig. 2 we have plotted the frequency dependence of the local DOS at a next-nearest-neighbor (NNN) site of the im-

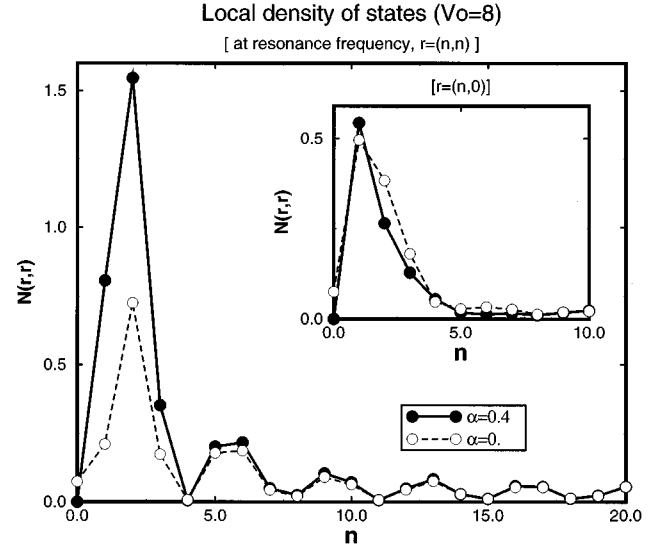


FIG. 3. Distance dependence of the local DOS at the resonance frequency $\omega = +\omega_{\text{res}}$ along the diagonal (main figure) and horizontal (insert) direction away from the impurity center at $\mathbf{r} = (0,0)$.

purity center showing a sharp resonance at a low subgap frequency ω_{res} . The p -wave scattering channels are too weak to contribute an additional structure and the single resonance has a mixed origin in the s - and d -wave channels. Quite remarkably, at this NNN site the strength of the resonance is enhanced by a factor 4 when α is increased from 0 to 0.4. Comparably weaker resonances at $\pm\omega_{\text{res}}$ with weaker α induced changes appear along the $(1,0)$ and $(0,1)$ direction and this anisotropy directly reflects the nodal structure of the $d_{x^2-y^2}$ gap function.^{10,11,13}

In Fig. 3 we show the oscillatory distance dependence of the local DOS along the diagonal (and, in the inset, horizontal) direction at the resonance frequency $\omega = \omega_{\text{res}}$. The enhancement due to a finite range of the potential is largest near the impurity center where the resonance is strongest. In comparing the results for the diagonal and the horizontal direction we recognize that the direction dependence of the resonant structure is amplified by the finite potential range thereby improving the possibility for detecting the anisotropic local DOS structure by STM in the vicinity of the impurity.

While this is already a very promising result for local experimental techniques we extend the algebraic results for the single extended impurity to a finite impurity concentration n_i within the self-consistent T -matrix (SCT) approximation. In the SCT approximation we obtain the impurity position averaged self-energy as $\hat{\Sigma}(\mathbf{k}, \omega) = n_i \hat{T}_{\mathbf{k},\mathbf{k}}(\omega)$. With $\hat{G}(\mathbf{k}, \mathbf{k}, \omega) = [(\hat{G}_0(\mathbf{k}, \omega))^{-1} - \hat{\Sigma}(\mathbf{k}, \omega)]^{-1}$ replacing \hat{G}_0 in the above exact formulas for the single impurity T matrix we solve the resulting self-consistency equations for \hat{G} by iteration without the usual assumption of particle-hole symmetry. Note that $\hat{\Sigma} = \sum_{i=0,1,3} \hat{\Sigma}_i \hat{\tau}_i$, i.e., the τ_1 component of the self-energy is finite for $\alpha > 0$.

Figure 4 shows the expected result for the SCT DOS for a low impurity concentration $n_i = 1\%$. At first sight the zero frequency DOS increase with turning on α might seem weak. However, within the chosen parametrization $\alpha = 0.5$ translates into $V_1/V_0 = 1/16$; i.e., if the NN impurity poten-

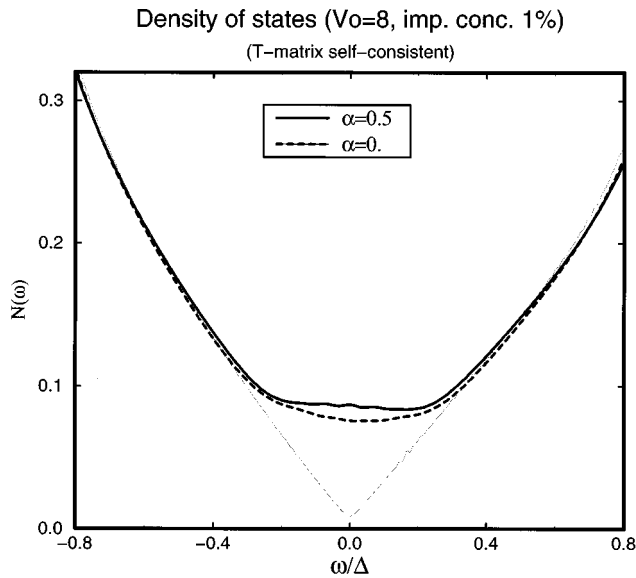


FIG. 4. Impurity position averaged DOS from the self-consistent T -matrix approximation for an impurity concentration of $n_i=1\%$. For the meaning of the different lines, see Fig. 2.

tial strength is only 6% of the impurity center value and accompanied by a suppression of the hopping amplitude to the impurity center, $N(\omega=0)$ increases by $\sim 15\%$ which is indeed significant.

In summary, we have solved a physically motivated extended impurity potential model in a $d_{x^2-y^2}$ superconductor. The finite range of the potential is argued to be dynamically generated around a local impurity from strong electronic correlations in the host system and thus relevant for high- T_c superconducting materials. While the model itself describes a static potential with a selected parameter relation it has the advantage to allow for an algebraic solution by decomposition into s -, p -, and d -wave scattering channels. The significant enhancements of the impurity-induced resonances by the finite potential range clearly improve the proposed possibility for probing the highly anisotropic local DOS structure near the impurity by STM experiments and may thus serve as an alternative fingerprint of the gap symmetry in cuprate and other unconventional superconductors. Furthermore, due to the physical relevance for the description of impurity effects in high- T_c superconductors some of the previous model studies with s -wave scattering from local impurity potentials may be reconsidered for the effects of an extended potential range for which the presented model can serve as an algebraically tractable tool.

A.P.K. acknowledges support through the Deutsche Forschungsgemeinschaft (DFG). A.P.K.'s research was performed within the program of the Sonderforschungsbereich 341 supported by the DFG. T.P.D. would like to acknowledge helpful discussions with Dr. J. Byers and Dr. M.E. Flatté.

¹P. W. Anderson, Phys. Rev. Lett. **3**, 325 (1959).

²J. Annett, N. Goldenfeld, and A. J. Leggett, in *Physical Properties of High Temperature Superconductors*, edited by D. M. Ginsberg (World Scientific, Singapore, in press), Vol. 5.

³J. F. Annett *et al.*, Phys. Rev. B **43**, 2778 (1991); P. J. Hirschfeld and N. Goldenfeld, *ibid.* **48**, 4219 (1992).

⁴P. J. Hirschfeld *et al.*, Phys. Rev. B **50**, 10 250 (1994).

⁵A. V. Balatsky *et al.*, Phys. Rev. Lett. **73**, 720 (1994).

⁶W. Hardy *et al.*, Phys. Rev. Lett. **70**, 3999 (1993); J. E. Sonnier *et al.*, *ibid.* **72**, 744 (1994).

⁷K. Ishida *et al.*, J. Phys. Soc. Jpn. **62**, 2803 (1994); T. Hotta, *ibid.* **62**, 274 (1993).

⁸T. P. Devereaux, Phys. Rev. Lett. **74**, 4313 (1995).

⁹L. Yu, Acta Phys. Sin. **21**, 75 (1965); H. Shiba, Prog. Theor. Phys. **40**, 435 (1968); A. I. Rusinov, Sov. Phys. JETP **9**, 85 (1969).

¹⁰J. M. Byers *et al.*, Phys. Rev. Lett. **71**, 3363 (1993); M. E. Flatté *et al.* (unpublished).

¹¹C. H. Choi, Phys. Rev. B **50**, 3491 (1994).

¹²A. V. Balatsky *et al.*, Phys. Rev. B **51**, 15 547 (1995).

¹³M. I. Salkola *et al.*, Phys. Rev. Lett. **77**, 1841 (1996).

¹⁴I. Maggio-Aprile *et al.*, Phys. Rev. Lett. **75**, 2754 (1995).

¹⁵G. Xiao *et al.*, Phys. Rev. B **42**, 8752 (1990); A. Mahajan *et al.*, Phys. Rev. Lett. **72**, 3100 (1994).

¹⁶T. R. Chien *et al.*, Phys. Rev. Lett. **67**, 2088 (1991); Y. Zhao *et al.*, J. Phys. Condens. Matter **5**, 3623 (1993).

¹⁷N. Bulut *et al.*, Phys. Rev. Lett. **62**, 2192 (1989).

¹⁸D. Poilblanc *et al.*, Phys. Rev. Lett. **72**, 884 (1994); Phys. Rev. B **50**, 13 020 (1994); W. Ziegler *et al.* (unpublished).

¹⁹T. Xiang and J. Wheatley, Phys. Rev. B **51**, 11 721 (1995).

²⁰P. J. Hirschfeld *et al.*, Phys. Rev. B **37**, 83 (1988).